From the Isolated Molecule to Oligomers and the Crystal: A Static Density Functional Theory and Car−Parrinello Molecular Dynamics Study of Geometry and Potential Function Modifications of the Short Intramolecular Hydrogen Bond in Picolinic Acid *N*-Oxide

Jarosław Panek,† Jernej Stare, and Dušan Hadži*

National Institute of Chemistry, Hajdrihova 19, SI-1000 Ljubljana, Slovenia

Received: January 30, 2004; In Final Form: June 16, 2004

The difference between the calculated metric parameters that are characteristic of the hydrogen bond (H-bond) in the isolated title compound and ones obtained from diffractions on crystals are unusually large (∼0.1 Å) even if high levels of theory are used. The probable origin of this discrepancy lies in strong intermolecular interactions that are investigated here using two models. The first one is the periodic density functional theory (DFT) with plane-wave basis sets and relativistic pseudopotentials (Car−Parrinello molecular dynamics, CPMD 3.5 program). An isolated molecule was also treated by this approach to facilitate the comparison with the local basis set model. The metric parameters calculated by the periodic model are in acceptable agreement with diffraction data, except for the O−H bond length. However, accounting for the quantum nature of the proton brought further improvement. The second model consisted of clusters of *n* molecules up to $n = 3$. With increase in the cluster size, the calculated geometry approached the experimental one. One-dimensional proton potential functions were calculated with the cluster and the periodic models. The effects of aggregation are markedly reflected in the shapes of the respective functions in that the increasing number of aggregated molecules tends to flatten the potential. The O−H stretching frequencies calculated from the potentials move to lower values with increasing aggregation. The frequency calculated for the crystal phase (1407 cm^{-1}) is in accord with the estimated center of the broad absorption appearing in the crystal spectrum. To obtain insight into the origin of the effects of molecular aggregation, we applied the natural bond orbital analysis [Reed, A. E.; Curtiss, L. A.; Weinhold, F. *Chem. Rev.* **1988**, *88*, 899−926]. The results suggest that the energy of association that is in the range of 3−5 kcal/mol originates in mutually induced charges.

1. Introduction

The predictive propensity of theoretical methods is gaining importance in modeling of matter that is involved in the various directions of new material design.[1] The treatments of intermolecular forces and their effects on the modifications of metric parameters and other molecular properties caused by aggregation are of particular importance for material design. In aggregates mediated by hydrogen bonds, the effects on aggregated molecules may be particularly dramatic as, for example, on the crystallization of carboxylic acids.[2] In contrast, one expects that intramolecular hydrogen bonds are much less involved in various types of changes inprinted upon aggregation. Indeed, in the example of benzoylacetone, the ab initio optimized metric parameters of the isolated molecule closely correspond to ones obtained from crystal diffractions.[3] Such similarity is not a rule, and examples of large differences between calculated gas-phase metric parameters and ones obtained from crystal diffractions are a challenge for theoretical methods developed for the prediction of crystal structure and dynamics.

While the prediction by well established ab initio and density functional theory (DFT) procedures of metric parameters[4] and other physical characteristics of isolated molecules and small clusters is at a mature stage, there is less of published experience in predictions of various parameter modifications caused by phase transitions and medium effects. However, it is just the bulk matter properties that are of prime practical interest, and with this, the prediction methods of molecular changes on aggregation are gaining importance. Illustrative of the need to carry out modeling by theoretical methods beyond the isolated molecules are the examples of orthoboric acid[5] and squaric acid,[6] as well as urea−phosphoric acid[7] and pyridine−methanesulfonic acid[8] complexes.

In our investigation of the structure and H-bond dynamics of picolinic acid *N*-oxide (PANO, Figure 1) and some of its substitution analogues,[9] we noted a large discrepancy between the energy-optimized metric parameters of the isolated PANO and the parameters obtained from X-ray[10] and neutron diffractions (ND)[11] (see Table 1). For instance, even when using fairly high levels of theory, the intramolecular O···O distance differed substantially (by ∼0.1 Å) from the experimental one. Improvements reached by applying the self-consistent reaction field solvent model (SCRF)[26] and explorative calculations on small clusters suggested that the source of discrepancies may lie in the effects of strong intermolecular interactions rather than in the use of inadequate level of theory. The results of the solvent effects as treated by the SCRF model are reported in ref 9; a comparison between the SCRF and Car−Parrinello molecular

* To whom correspondence should be addressed. E-mail: dusan.hadzi@ki.si.

† Permanent address: Faculty of Chemistry, University of Wrocław, F. Joliot-Curie 14, PL-50383 Wrocław, Poland.

10.1021/jp0495794 CCC: $27.50
Published on Web 08/18/2004

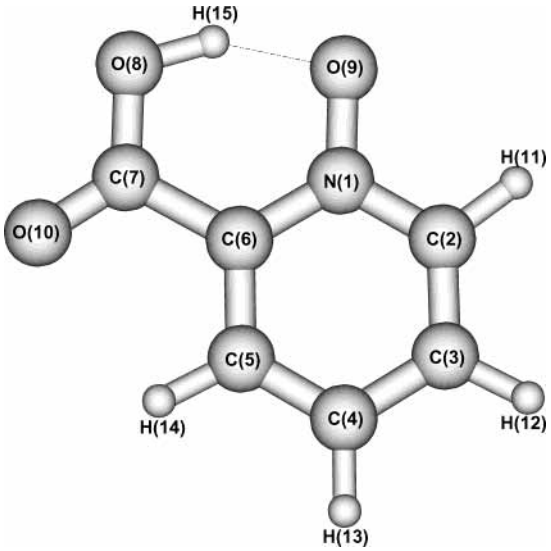

Figure 1. The structure of picolinic acid *N*-oxide (PANO) and atomic labels.

TABLE 1: Selected Interatomic Distances (in Å) in Energy-Minimized PANO Monomer in the Gas Phase Calculated at Various Levels of Theory

level of theory	O···O	O−H	O···H	N−O
B3LYP/6-31+G(d,p)	2.509	1.011	1.567	1.308
B3LYP/6-311+G(d,p)	2.519	1.004	1.588	1.301
B3LYP/6-311++G(3df,3pd)	2.507	1.006	1.569	1.299
B3LYP/cc-pVTZ	2.509	1.007	1.570	1.298
MP2/6-31+G(d,p)	2.521	1.007	1.582	1.300
MP2/6-311+G(d,p)	2.513	1.002	1.572	1.285

dynamics (CPMD) predictions is made in the Results and Discussion section.

To clarify the quandary of the metric parameters and other H-bond characteristics, we extended the initial computations by applying plane-wave basis sets and periodic boundary conditions, as implemented in the CPMD program.[12,13] The resulting metric parameters confirmed the supposition that the proper accounting of intermolecular effects brings the metric parameters quite close to the experimental values.

The short O···O distance (2.425 Å, ref 10) in PANO raises interest in calculations of other H-bonding characteristics besides the metric parameters. Of prime interest are the proton dynamics and its reflections in the vibrational frequencies. In this respect, PANO and its substitution analogues are very attractive because they are among the exceptional compounds with extremely short intramolecular H-bonds without formal charge. The absorption due to the OH stretching in the infrared spectra of PANO in several solvents was located.[9] This is a challenge for the calculation of proton potential surfaces, vibrational energy levels, and the effects of environment.[14] Complementary to the earlier calculations on isolated PANO and its solutions,[9] we pursued in this work the effects of clustering on the O−H stretching frequency.

The remarkably large effects of molecular aggregation on clusters and crystals raise the question of the origin of intermolecular forces. This we investigated by an analysis based on the natural bond orbitals (NBO)[15] that can readily be applied in various flavors for studies of hydrogen-bonded systems.[16,17] We treated PANO monomer, dimer, and trimer at the B3LYP/6-31+G(d,p) level of theory. The results show clearly that the aggregation effects on metric parameters and local charges increase with the size of the cluster.

TABLE 2: Selected Interatomic Distances (in Å) in PANO Calculated by the Cluster and Periodic Approaches (See Text) and the Corresponding Experimental Values[a]

	O···O	O−H	O···H	N−O	N···H
B3LYP/6-31+G(d,p); Gaussian 98					
monomer	2.509	1.011	1.567	1.308	
dimer	2.489	1.018	1.533	1.315	3.140
trimer	2.469	1.027	1.496	1.321	3.216
BLYP/6-31+G(d,p); Gaussian 98					
monomer	2.535	1.026	1.574	1.324	
dimer	2.515	1.033	1.540	1.329	3.394
trimer	complex not stable (dissociation)				
BLYP/PW; CPMD 3.5					
monomer	2.527	1.027	1.561	1.326	
crystal Γ-point	2.451	1.061	1.426	1.355	3.040
crystal, partial opt. with *k*-points	2.463	1.061	1.447	1.351	3.040
Neutron Diffraction[b]					
	2.426	1.091	1.374	1.342	3.037

[a] Note that the N···H (stacking) distance corresponds to molecules in two adjacent layers. Listed values for the trimer pertain to the central molecule (see also Figure 2). [b] Reference 11.

2. Computational Section

Periodic Plane-Wave Treatment. Geometry optimizations were performed with the BLYP density functional coupled with a plane-wave basis set with energy cutoff of 120 Ry and relativistic Goedecker pseudopotentials[18] as implemented in the Car−Parrinello Molecular Dynamics (CPMD, version 3.5) program.[13] Note that hybrid density functionals such as the popular B3LYP are not supported by CPMD since calculations of the exact exchange energy as required by the functional are far beyond the normal computing capabilities in the plane-wave basis set. Periodicity of the system was fully taken into account. The unit cell of a monoclinic type (space group $P2_1/m$, $a = 6.802$ Å, $b = 6.066$ Å, $c = 7.804$ Å, $\beta = 112.61°$, two PANO molecules in the unit cell) was modeled according to the crystallographic data.[10] Complete geometry optimization was performed within Γ-point approximation. Since the PANO molecules interact via C−H···O and stacking interactions, much weaker than the discussed O−H···O bond, this approximation is reasonable. Indeed, a $2 \times 2 \times 2$ Monkhorst−Pack *k*-point optimization yields only small changes with respect to the Γ-point result (see Table 2). However, the *k*-point optimization did not converge fully, and in view of its apparently minor impact on the structure, the Γ-point values will be discussed further. Besides the fully periodic system, we also applied this methodology to the isolated PANO molecule.

Calculations on Clusters. Geometry optimizations within the cluster approach included monomer, dimer, and trimer of PANO at the B3LYP/6-31+G(d,p) level of theory. Test calculations on PANO monomer with larger and more flexible basis sets, as well as with the MP2 method, show no significant improvement in the optimized geometry relative to B3LYP/6-31+G(d,p) (see Table 1). Thus we adopted the latter for our calculations since it offers a good compromise between CPU economy and reliability. To enable direct comparison between periodic and cluster treatment, we also present the results obtained by the BLYP functional combined with the 6-31+G(d,p) basis set in cluster calculations. Individual PANO molecules in the initial structures of dimers, trimers, and the crystal were aligned according to the crystallographic data. Dimers and trimers were constructed to preserve the N···H stacking interaction between two molecules of PANO in the adjacent layers

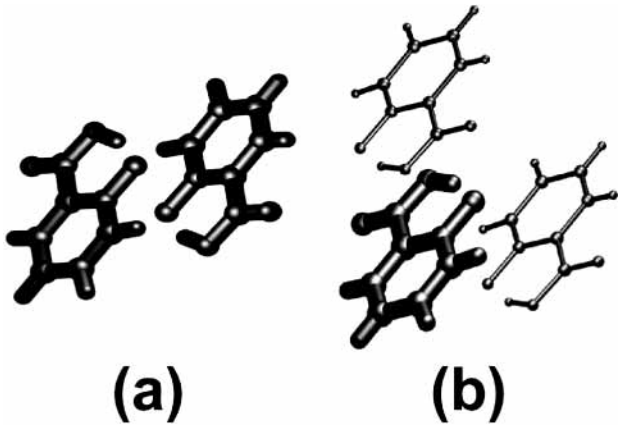

Figure 2. Picolinic acid *N*-oxide dimer (a) and trimer (b).

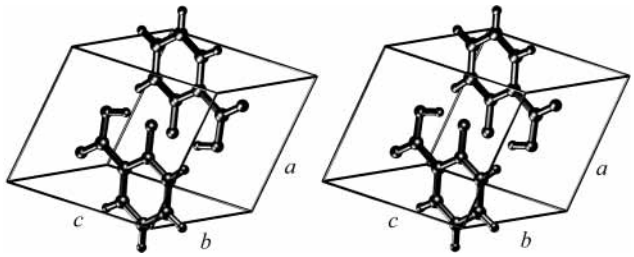

Figure 3. Stereographic view of the unit cell of picolinic acid *N*-oxide.

(see Figures 2 and 3). Calculations within this approach were performed with the Gaussian 98[19] suite of programs.

Calculation of Proton Potentials. For all the above-mentioned models, we constructed one-dimensional potential energy functions in the following way. The proton was allowed to move along the circular arc defined by the donor and acceptor oxygen nuclei and the hydrogen nucleus in the optimized structure. All the other nuclei in the molecule were kept in their equilibrium positions. The circular arc as described above is, most likely, a simplification of the real motion. However, it is justified by the results of elaborate studies of proton-transfer paths in malonaldehyde.[20] We allowed the proton to be resident at 45 uniformly spaced points along the arc with the additional restriction that the distance to the nearer oxygen atom be larger than 0.75 Å. This condition typically reduced the number of proton positions included in the calculation of the potential energy function to about 16−18. In cases of dimeric, trimeric, and crystalline structures, all the H-bonded protons were moved simultaneously. This allowed for a consistent calculation of the potential energy per one PANO molecule. Test calculations have shown that the proton motions in adjacent molecules (both in the crystal and in clusters) practically do not interfere. Thus the chosen model is justified. Moreover, it is the sole one that allows economic calculations. The procedure for calculating proton positions is available from the authors on request.

Anharmonic O−H Stretching Frequencies and Expectation Values of the O−H Distance. We solved the one-dimensional time-independent vibrational Schrödinger equation in the calculated potential by means of the program package developed in this laboratory,[21,22] yielding anharmonic vibrational energy levels and their proton wave functions. A sample case is displayed in Figure 5. In addition, we have calculated the anharmonic O−H stretching frequency and the ground-state expectation value of the O−H distance in each given case.

In the calculation of proton potentials, we fixed all the nuclei except the H-bonded proton in their equilibrium positions rather than relaxing them by partial geometry optimization to follow the proton in a minimum energy path. The choice of this strategy is supported both by recent three- and four-dimensional anharmonic studies on malonaldehyde[23,24] and by our experience with anharmonic frequencies of OHO moieties of short H-bonds derived from one- and two-dimensional potential energy surfaces.[22] While the OH stretching frequencies yielded by models in which the nuclear positions are optimized for each proton position are typically too low with respect to experimental data,[23] the agreement is much better when these nuclei are kept fixed in their equilibrium positions.[24] Besides, the strategy we applied is computationally much less expensive than the one with partial geometry optimization in each point of proton potential evaluation.

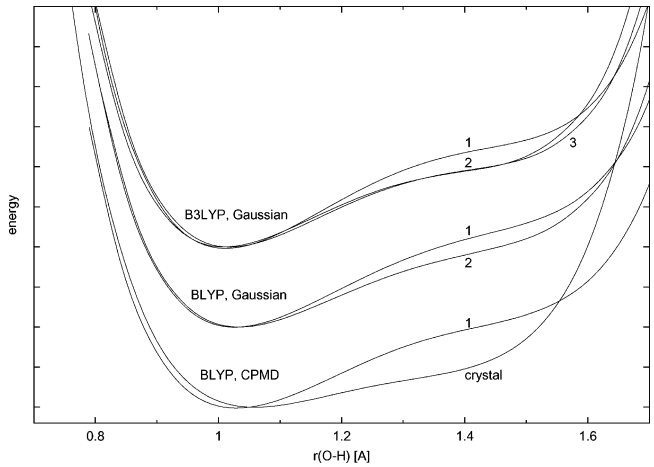

Figure 4. Proton potential energy functions of different models of picolinic acid *N*-oxide calculated by the programs indicated (i.e., Gaussian 98 or CPMD v. 3.5): (1) monomer; (2) dimer; (3) trimer; (crystal) fully periodical model). The functions are groupped according to the level of theory and shifted to avoid overlapping. The interval on the *y* axis corresponds to 5 kcal/mol.

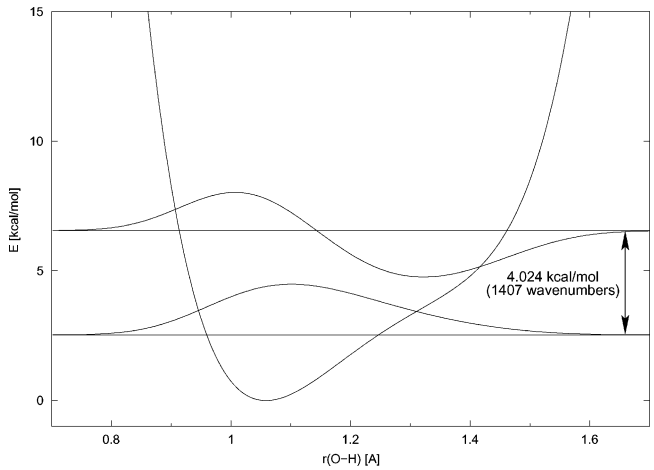

Figure 5. Proton potential energy function of the "crystal" model of picolinic acid *N*-oxide together with its two lowest vibrational levels and proton wave functions. The O−H stretching excitation energy of 1407 cm^{-1} is indicated.

NBO Analysis. We modeled a dimer and trimer of PANO using the B3LYP/6-31+G(d,p)-optimized monomers and assembling them in the stacked structure (Figures 2 and 3) as described above. We performed a B3LYP/6-31+G(d,p) single-point calculation, followed by the natural bond orbital (NBO) analysis (version 3.1, included in the Gaussian 98 program package), on each of the so-constructed clusters, yielding natural atomic and molecular orbitals, atomic charges, and bond−antibond interaction energies in the NBO basis.

3. Results and Discussion

Metric Parameters. Comparison of the H-bond characterizing calculated metric parameters with the diffraction data (Table 1) shows large differences between both sets in that the calculated O···O and O···H distances are much longer than ones derived from X-ray or neutron diffractions,[10,11] while the opposite is true of the O−H bond length. The discrepancies are practically independent of the level of theory.

Considering the metric parameters of the clusters, essential approaching to the crystal parameters is achieved with the number of PANO molecules included in the model as shown in Table 2. The O···O distance, which is, aside from the O−H, the most characteristic metric parameter of the hydrogen bond, is in the monomer in obvious disaccord with the experimental value, exceeding it by as much as 0.1 Å in the BLYP-treated monomers. The O−H distance is underestimated especially when considering the fact that the X-ray-determined O−H distance of 1.041 Å is also shorter than the more reliable neutron diffraction result of 1.091 Å. Consequently, the O···H distance is in an even worse clash with the experimental value than the O···O distance. Regarding the cluster approach, the B3LYP functional seems to yield lower O···O distances than the BLYP; however, the latter yields longer O−H and N−O distances that are in somewhat better agreement with the experiment than those obtained by the B3LYP functional. It seems that the BLYP functional underestimates, relative to B3LYP, the stacking interaction between PANO molecules of the adjacent layers. Note that we use the term "stacking" in a broader sense than usual (i.e., vertical ordering of aromatic rings). The B3LYP interlayer N···H distance in the PANO dimer, reported in the table, is much shorter than that of BLYP (3.140 vs 3.394 Å) and thus closer to the experimental value of 3.037 Å. This result is reflected by the considerable difference in the estimated dimerization energy, which equals 4.99 kcal/mol for B3LYP and only 3.52 kcal/mol for BLYP, and, moreover, by the fact that the BLYP trimer structure could not be optimized but led to disintegration. This, however, poses no problems in the periodic approach, since the unit cell parameters are fixed to the crystallographic values.

It is important to note that the BLYP/6-31+G(d,p) monomer geometry is very close to one resulting from the BLYP/PW calculation (Table 2), suggesting consistency in accuracy between the two respective basis sets. This was very recently shown to be so in the example of Vienna ab initio simulation package (VASP) calculations on a series of test molecules.[25] A very significant shift in equilibrium geometry is achieved by applying full periodicity. The O···O distance shrinks by no less than 0.076 Å and differs from the experimental one by only 0.026 Å. Note also the extension of the O−H and N−O distances. On the whole, the full periodic geometry optimization yields acceptable agreement with the experimental structure. Nevertheless, there is still scope for improving on the O−H bond length by taking into account the quantum nature of the H-bonded proton (see below).

Proton Potentials and Anharmonic O−H Stretching Frequencies. The shape of the proton potential energy functions and the pertinent vibrational energy levels (Figure 4 and Table 3) reveal that BLYP yields flatter potentials than B3LYP and, consequently, lower vibrational zero points and lower anharmonic O−H stretching frequencies. The shape of the potential exhibits in general significant deviations from harmonicity. The calculated harmonic frequencies are in the range of 2900 cm^{-1}, which seems to be far off the values expected with such a short H-bond. Comparing the BLYP-calculated anharmonic O−H stretching frequencies for a single PANO molecule model (i.e., localized vs plane-wave basis set), one observes quite a pronounced difference between both approaches. The former yields the frequency of 2099 cm^{-1}, while the latter results in 1904 cm^{-1}, which is closer to the frequency yielded for the PANO dimer in the cluster model (1896 cm^{-1}). This suggests that the curvature of the potential is much more sensitive to the level of calculation than the optimized geometry. Comparison of the anharmonic O−H stretching frequencies within the given level of theory suggests the same conclusion as in the case of optimized geometry—the larger the cluster, the lower (and closer to infrared experimental findings) the frequency. The striking similarity of the frequencies resulting from the periodic treatment of PANO and ones from the experimental spectra of solutions[9] may be fortuitous; the width and the shape of the experimental absorption do not permit, in fact, the attribution of a precise frequency to the OH stretching. However, the absence of specific interactions between the molecules in the crystal may explain the similarity between the effects of the crystal and of the polar solvents. Calculations of the effect of the latter on the optimized metric parameters support this assumption. The effect of acetonitrile ($\epsilon = 36.6$) as accounted for by the SCRF model[26] reduces the O···O distance to 2.464 Å, a value very similar to the one obtained for the crystal model. The location of the ν_{OH} absorption in dissolved PANO is more reliable than that in the solid. In the latter, the absorption is heavily smeared out; the center can be estimated to ∼1500 cm^{-1}.[9] Assignment of the O−H stretching and deformation modes in the infrared spectra of PANO and derivatives has been proposed by Szafran and co-workers[27] and by Zundel and co-workers;[28] they differ from the present one and will be discussed elsewhere.[29]

Clearly the one-dimensional potential is a simplification in calculating the OH stretching frequency. With a model based on the two-dimensional potential energy surface with O···O stretching as the second dimension resulted in $\nu_{OH} = 1733$ cm^{-1}.[21] With O−H bending as the second dimension, the value of 1299 cm^{-1} was obtained.[22] These frequencies are not too far off the result obtained with the one-dimensional potential, particularly when considering the fact that the experimental absorptions are very broad and thus the exact ν_{OH} frequency (in fact, the high-frequency component of the complex OHO absorption[24]) not well defined. Moreover, we have calculated for a series of molecules with a short intramolecular H-bond

TABLE 3: Calculated Anharmonic O−H Stretching Infrared Frequencies (ν_{OH} in cm^{-1}) and Ground-State Expectation Values of the O−H Distance (⟨OH⟩ in Å) of PANO Obtained from the Solution of the Vibrational Schrödinger Eqauation in the Previously Calculated Potential Energy Function[a]

	ν_{OH}	⟨OH⟩
B3LYP/6-31+G(d,p); Gaussian 98		
monomer	2232	1.046
dimer	1975	1.059
trimer	1957	1.050
BLYP/6-31+G(d,p); Gaussian 98		
monomer	2099	1.063
dimer	1896	1.075
BLYP/PW; CPMD 3.5		
monomer	1904	1.068
crystal	1407	1.124
Experimental Values		
crystal	∼1500[b]	1.041,[c] 1.091[d]

[a] Experimental values of the O−H distance, obtained by X-ray and neutron diffraction, are also listed. [b] Estimated frequency. [c] X-ray diffraction (ref 10). [d] Neutron diffraction (ref 11).

the so-called ν_{OH} frequencies beyond the harmonic approximation using the vibrational self-consistent field method.[30] The results are not satisfying if comparison with the experimental spactra is made (these results with appropriate comments will be published separately[29]). For the present results obtained with the one-dimensional potential, it can be said that the comparison with experiment is satisfying despite the adopted simplifications thus justifying the application of this potential.

Since neutron diffractions are superior to ones of X-rays for determining the proton position, we take the ND-determined O−H bond length of 1.091 Å for reference and find out that all the optimized values for this distance are much too short. Even with the fully periodic model, which best matches the experimental structure, we obtained a value of only 1.061 Å. Taking into account the quantum nature of the proton and knowing that the proton potential energy function is highly anharmonic and thus the proton wave function asymmetric, we can expect some elongation of the O−H distance when taking it as an expectation value by the equation (note that $\psi(x)$ is always real in our case)

$$\langle \mathrm{OH} \rangle = \int \psi(x) x \psi(x)\, \mathrm{d}x$$

where $x \equiv$ O−H distance and $\psi(x)$ is the ground-state proton wave function. The expectation values, listed in Table 3, are indeed by at least 0.03 Å longer than the O−H distance in the corresponding optimized geometry. The elongation is larger for flatter potentials; with the full periodic model, we obtained a somewhat exaggerated value of 1.124 Å, a 0.063 Å elongation of the equilibrium O−H distance.

NBO Analysis. The NBO analysis reveals some clues for the interaction between the molecules of PANO in the crystal phase. To get comparable results, we studied the monomer, dimer, and trimer, which were made up of individual PANO molecules of exactly the same geometry, which is the one obtained by the B3LYP/6-31+G(d,p) geometry optimization of a single PANO molecule in the gas phase. The most interesting part of the analysis is the bond−antibond stabilization interactions in the NBO basis due to electron delocalization from some occupied (bond or lone pair) NBO into an empty or partially occupied antibond NBO. The interaction energy is calculated by means of second-order perturbation theory for each possible pair of donor and acceptor NBOs and results in charge changes. In the example of PANO, there are many such interactions that are energetically important and exceed 10 kcal/mol; many of them correspond to charge delocalization within the aromatic ring. None of the orbital interactions with the acceptor NBO residing in a different PANO molecule than the donor NBO is energetically important; this suggests that the interactions between individual PANO molecules do not include significant contributions of intermolecular electron delocalization and are thus mainly of electrostatic origin.

The most interesting interactions between the NBOs are those involved inside or near to the O−H···O moiety; two of them are significantly dependent on whether the molecules of PANO are monomeric, dimeric, or trimeric. They are (see Figure 6) (a) delocalization of the lone pair on O(9) into the π antibond orbital between N(1) and C(6) and (b) delocalization of the lone pair on O(9) into the σ antibond orbital between O(8) and H(15). The stabilization energies in monomeric, dimeric, and trimeric PANO for the above cases are listed in Table 5. These interactions are significant since the stabilization energy always exceeds 30 kcal/mol (note that this is an intramolecular energy effect). When the cluster is increased by adding PANO molecules, interaction a is weakened and interaction b is enhanced. The change in the interaction energy is about −1.3 kcal/mol per added molecule of PANO in interaction a and about 0.9 kcal/mol in interaction b; this change is slightly smaller when moving from dimer to trimer relative to the case of passing from monomer to dimer.

The observed changes in the above interactions are synergetic and support the assumption that the hydrogen bond strength (as reflected in the O···O distance) is enhanced with increasing cluster size. Namely, when lone pair electrons on O(9) are more strongly delocalized into the O−H antibond (interaction b), they are less readily available for delocalization into the aromatic ring (interaction a). Apart from the above cases, there are many other interactions that exhibit dependence on the number of PANO molecules in the cluster, but the change in the interaction

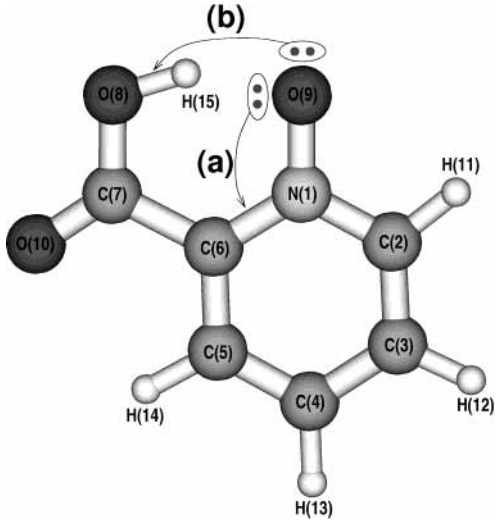

Figure 6. Selected lone pair−antibond electron delocalizations (in the NBO basis) in picolinic acid *N*-oxide: (a) delocalization of the lone pair on O(9) into the π antibond orbital between N(1) and C(6); (b) delocalization of the lone pair on O(9) into the σ antibond orbital between O(8) and H(15). See text for explanation.

TABLE 4: Natural Charges of PANO Monomer, Dimer, and Trimer

	natural charge		
nucleus	momomer	dimer	trimer
N(1)	+0.052	+0.046	+0.036
C(2)	+0.035	+0.050	+0.065
C(3)	−0.199	−0.198	−0.197
C(4)	−0.186	−0.180	−0.175
C(5)	−0.167	−0.168	−0.170
C(6)	+0.074	+0.084	+0.094
C(7)	+0.769	+0.776	+0.783
O(8)	−0.666	−0.681	−0.696
O(9)	−0.562	−0.578	−0.596
O(10)	−0.587	−0.589	−0.590
H(11)	+0.234	+0.239	+0.244
H(12)	+0.228	+0.229	+0.229
H(13)	+0.223	+0.222	+0.221
H(14)	+0.256	+0.254	+0.253
H(15)	+0.495	+0.494	+0.493

TABLE 5: Selected NBO Bond−Antibond Interaction Energies (in kcal/mol)[a]

	NBO interaction energy		
donor and acceptor NBOs	momomer	dimer	trimer
(a) $n_{O(9)} \rightarrow \pi^*_{N(1)-C(6)}$	39.97	37.67	35.59
(b) $n_{O(9)} \rightarrow \sigma^*_{O(8)-H(15)}$	38.16	39.06	39.90

[a] See text for explanation.

energy is much smaller, being in the range of a few hundreths to a few tenths of a kilocalorie per mole per added molecule of PANO. Importantly, all the changes in delocalization energies in these cases are in accord with the assumption that the strength of the hydrogen bond increases with increasing the number of PANO molecules contained in the cluster. Eventually, the consequences of those observations result in geometry optimization of a cluster of PANO molecules: due to the enhanced proton donor/acceptor interaction, the O−H and the N−O distances are elongated, while the O···O distance is shortened, shifting the structure closer to the experimental values.

Similar conclusions can be drawn by comparing the natural atomic charges in the monomer, dimer, and trimer (see Table 4). Most sensitive to clustering are the donor and acceptor oxygens; there is a substantial increase of negative charge on both O(8) and O(9) upon di- or trimerization, which is well-known to be an effect that enhances the strength of a hydrogen bond. Apart from O(8) and O(9), the carboxylic carbon C(7), the nitrogen N(1), and the next-lying ring carbons, C(2) and C(6), also exhibit a notable dependence of natural atomic charges on the size of the cluster. Among these, C(2) is particularly interesting since the considerable change of its natural charge with the number of molecules in the cluster is somewhat unusual because it is not located in the closest vicinity of the O−H···O moiety. However, in clusters of two or more PANO molecules, C(2) is relatively close to the oxygen atom of the O−H group of the adjacent molecule (see Figure 3); hence this dependence may well be due to polarization. Accordingly, the charge of the ring hydrogen H(11) that is directly attached to C(2) and thus also near to O(8) of the neighbor molecule of PANO also exhibits a significant dependence on the cluster size.

4. Conclusions

We have studied the influence of intermolecular interactions on the hydrogen bond in picolinic acid *N*-oxide (PANO), as reflected in the equilibrium geometry, the shape of the proton potential energy function, and the anharmonic O−H stretching excitation energies. We modeled our system in two distinct ways. Within the cluster approach, we modeled small isolated clusters (dimers and trimers, as well as monomers) of PANO, treating them using density functional theory (DFT), coupled with localized Gaussian-type basis sets. Alternatively, we used the periodic approach, in which we fully took into account the periodicity of the system; we also treated an isolated molecule within this approach for better comparison. A periodic DFT coupled with plane-wave basis sets and relativistic pseudopotentials was used for this purpose. Anharmonic vibrational levels and wave functions for a given proton potential were obtained by solving the vibrational time-independent Schrödinger equation.[21] We also performed a natural bond orbital (NBO) analysis to study the electron structure of monomer, dimer, and trimer of PANO. We compared the calculated metric parameters and vibrational frequencies to experimental data.[9−11]

Calculations on PANO monomer in the gas phase yielded, relative to diffraction data, too long O···O distance and too short O−H and N−O distances. Although small differences between experimental and calculated geometries may emerge due to the effect of averaging over the vibrational states of the system that is essentially accounted for by diffraction techniques but not by calculations,[31] the differences in the present case are much too large to be explained only by the lack of taking into account the contribution of the excited vibrational states to the geometry in our calculations. The calculated anharmonic O−H stretching frequency also was considerably higher than the experimental one. The cluster calculations have shown that the more PANO molecules were included, the shorter became the O···O distance and the longer are the O−H and N−O distances in the optimized geometry thus improving the agreement with the experiment. Accordingly, the proton potentials are flattened and the resulting anharmonic frequencies lowered with increasing number of PANO molecules included in the model. Ultimately, the full periodic model and plane-wave calculations yielded an optimized geometry that was in very good agreement with the experimental data. Geometry corrections due to the quantum nature of the hydrogen-bonded proton even improved this agreement. The anharmonic O−H stretching frequency obtained within this model also matches very well the experimental one. The experience with the intramolecularly bonded PANO is in accord with one obtained by the same treatment of an example of intermolecular bonding, the pyridine *N*-oxide−trichloroacetic acid complex.[32]

NBO studies of the isolated PANO molecule and of its dimer and trimer have shown that some of the delocalization interactions between donor (bond, lone pair) and acceptor (antibond) NBOs are significantly dependent on the number of PANO molecules included in the model, in particular the interaction between the lone pair on the (N)−O oxygen and the σ^* (C)−O−H antibonding orbital. The observed trend supports the conclusion that the more molecules of PANO are included in the model, the shorter becomes the hydrogen bond. Corresponding conclusions can be made from the comparison of natural atomic charges in PANO monomer, dimer, and trimer.

To reach the present results, we used possibly inexpensive calculations. Thus one cannot expect particularly precise accords between theory and experiment. In the case of vibrational frequencies, the character of the infrared spectra of PANO and other systems with short intramolecular H-bonds (extreme broadening of the high-frequency OH absorption in the solid) is anyway not prone to quantitative work. The main purpose of the present work lays in seeking a compromise between possible computational models and computer time expenses to proceed to other examples of short intramolecular H-bonds with poorly understood vibrational spectra and also to a more detailed analysis of the vibrational spectra of PANO and its congeners.

Acknowledgment. Financial support from the Ministry of Education, Science and Sports of the Republic of Slovenia is gratefully acknowledged. Warm thanks are due to Dr. Janez Mavri, National Institute of Chemistry, Ljubljana, Slovenia, for many stimulating discussions and critical reading of the manuscript.

References and Notes

(1) Beyer, T.; Price, S. L. *J. Phys. Chem. B* **2000**, *104*, 2647−2655.
(2) Rovira, C.; Novoa, J. J. *J. Chem. Phys.* **2000**, *113*, 9208−9216.
(3) Schiøtt, B.; Iversen, B. B.; Madsen, G. K. H.; Bruice, T. C. *J. Am. Chem. Soc.* **1998**, *120*, 12117−12124.
(4) Márquez, J. S.; Núñez, M. F. *J. Mol. Struct. (THEOCHEM)* **2003**, *624*, 239−249.
(5) Zapol, P.; Curtiss, L. A. *J. Chem. Phys.* **2000**, *113*, 3338−3342.
(6) Rovira, C.; Novoa, J. J.; Ballone, P. *J. Chem. Phys*. **2001**, *115*, 6406−6416.
(7) Wilson, C. C.; Morrison, C. A. *Chem. Phys. Lett.* **2002**, *362*, 85−89.
(8) Lehtonen, O.; Hartikainen, J.; Rissanen, K.; Ikkala, O.; Pietilä, L.-O. *J. Chem. Phys.* **2002**, *116*, 2417−2424.
(9) Stare, J.; Mavri, J.; Ambrožič, G.; Hadži, D. *J. Mol. Struct. (THEOCHEM)* **2000**, *500*, 429−440.
(10) Steiner, T.; Schreurs, A. M. M.; Lutz, M.; Kroon, J. *Acta Crystallogr*. **2000**, *C56*, 577−579.
(11) Steiner, T. Unpublished work.
(12) Car, R.; Parrinello, M. *Phys. Rev. Lett.* **1985**, *55*, 2471−2474.

(13) *Car-Parrinello Molecular Dynamics*, version 3.5; Copyright IBM Corporation 1990−2004.

(14) Stare, J.; Jezierska, A.; Ambrožič, G.; Košir, I. J.; Kidrič, J.; Koll, A.; Mavri, J.; Hadži, D. *J. Am. Chem. Soc.* **2004**, *126*, 4437−4443.

(15) Reed, A. E.; Curtiss, L. A.; Weinhold, F. *Chem. Rev.* **1988**, *88*, 899−926.

(16) Reed, A. E.; Weinhold, F. *J. Chem. Phys.* **1983**, *78*, 4066−4073.

(17) Glendening, E. D.; Streetwieser, A. *J. Chem. Phys.* **1994**, *100*, 2900−2909.

(18) Hartwigsen, C.; Goedecker, S.; Hutter, J. *Phys. Rev.* **1998**, *B58*, 3641.

(19) Frisch, M. J.; Trucks, G. W.; Schlegel, H. B.; Scuseria, G. E.; Robb, M. A.; Cheeseman, J. R.; Zakrzewski, V. G.; Montgomery, J. A., Jr.; Stratmann, R. E.; Burant, J. C.; Dapprich, S.; Millam, J. M.; Daniels, A. D.; Kudin, K. N.; Strain, M. C.; Farkas, O.; Tomasi, J.; Barone, V.; Cossi, M.; Cammi, R.; Mennucci, B.; Pomelli, C.; Adamo, C.; Clifford, S.; Ochterski, J.; Petersson, G. A.; Ayala, P. Y.; Cui, Q.; Morokuma, K.; Malick, D. K.; Rabuck, A. D.; Raghavachari, K.; Foresman, J. B.; Cioslowski, J.; Ortiz, J. V.; Stefanov, B. B.; Liu, G.; Liashenko, A.; Piskorz, P.; Komaromi, I.; Gomperts, R.; Martin, R. L.; Fox, D. J.; Keith, T.; Al-Laham, M. A.; Peng, C. Y.; Nanayakkara, A.; Gonzalez, C.; Challacombe, M.; Gill, P. M. W.; Johnson, B. G.; Chen, W.; Wong, M. W.; Andres, J. L.; Head-Gordon, M.; Replogle, E. S.; Pople, J. A. *Gaussian 98*, revision A.7; Gaussian, Inc.: Pittsburgh, PA, 1998.

(20) Tautermann, C. S.; Voegele, A. F.; Loerting, T.; Liedl, K. R. *J. Chem. Phys.* **2002**, *117*, 1962−1966.

(21) Stare, J.; Mavri, J. *Comput. Phys. Commun.* **2002**, *143*, 222−240.

(22) Stare, J.; Balint-Kurti, G. G. *J. Phys. Chem. A* **2003**, *107*, 7204−7214.

(23) Babič, D.; Bosanac, S. D.; Došlić, N. *Chem. Phys. Lett.* **2002**, *358*, 337−343.

(24) Došlić, N.; Kühn, O. *Z. Phys. Chem.* **2003**, *217*, 1507−1524.

(25) Sun, G.; Kürti, J.; Rajczy, P.; Kertesz, M.; Hafner, J.; Kresse, G. *J. Mol. Struct. (THEOCHEM)* **2003**, *624*, 37−45.

(26) Tomasi J.; Persico, M. *Chem. Rev.* **1994**, *94*, 2027−2094.

(27) Dega-Szafran, Z.; Grundwald-Wyspianska, M.; Szafran, M. *J. Mol. Struct.* **1992**, *275*, 159−165.

(28) Böhner, U.; Zundel, G. *J. Phys. Chem.* **1986**, *90*, 964−973.

(29) Eckert, J.; Daemen, L.; Stare, J.; Spanget-Larsen, J.; Hadži, D., manuscript in preparation.

(30) Bowman, J. M. *Acc. Chem. Res.* **1986**, *19*, 202−208.

(31) Hargittai, M.; Hargittai, I. *Int. J. Quantum Chem.* **1992**, *44*, 1057−1067.

(32) Stare, J.; Merzel, F.; Hadži, D., manuscript in preparation.